CONSTRAINING IONIZATION AND ILLUMINATING PLANET FORMATION WITH ALMA AND JWST

Deryl Long[1] and Advisor: Ilse Cleeves[1]

[1] *University of Virginia*
530 McCormick Rd.
Charlottesville, VA 22903, USA

Abstract

Ionization plays a critical role in setting the chemical and dynamical processes within protoplanetary disks (PPDs). Ions are responsible for the most rapid chemical processes which govern the formation of organics and water in the cold midplane of the disk, making ionization-driven chemistry central to the chemical evolution of any planets that may be forming within it. Sufficient ionization also allows the gas to couple to magnetic field lines and in turn drives magneto-rotational instability (MRI). Regions in the midplane in which the disk is not MRI active ("dead zones") are thought to be safe havens for planet formation. Constraining the ionization fraction throughout a disk is crucial for understanding both possible planet compositions and planet-forming capabilities. We use ALMA observations of two ionization-tracing molecules (HCO^+ & N_2H^+) and a grid of 2D chemical models to constrain the ionization fraction in the DM Tau protoplanetary disk. We then explore the application of our methods to large surveys, laying the groundwork for future ionization studies that leverage the full power of both ALMA and JWST.

Introduction

Since the discovery of the first exoplanet in 1995, the number of known planets outside of our solar system has skyrocketed. Thousands of exoplanets have been detected and many of them characterized (Batalha 2014). We have evidence, including direct images, of planets forming in protoplanetary disks around young stars (Wang et al. 2020). This leads us to believe that planet formation happens often and there could be many potentially life-sustaining worlds in our Universe. Despite abundant proof of its occurrence, the mechanisms of planet formation and the disk properties that set planets' compositions are largely unconstrained.

Protoplanetary disks are composed of gas and dust particles that settle to the midplane of the disk over time. For planets to form, these dust particles must stick together to form aggregates and eventually planetesimals. The first stage of dust growth must happen efficiently in order to overcome radial drift and repulsion between charged dust particles (Okuzumi 2009). A promising mechanism for overcoming this "growth barrier" is turbulence due to magnetorotational instability (MRI; Balbus & Hawley (1991)). Dust in turbulent, or MRI-active, regions may stick together more efficiently than dust in "dead zones". However, too much turbulence could cause planetesimals to break apart more quickly than they can form (Weidenschilling & Cuzzi 1993). The amount of magnetohydrodynamic turbulence is set by the level of ionization– a property that allows disk material to couple to the magnetic field. Recent work by Speedie et al. (2021) shows a distinct bifurcation in outcomes for protoplanets in high and low turbulent viscosity disks. Thus, the steps for forming planets– from dust growth to oligarchic and atmospheric growth– are crucially sensitive to the level of ionization.

Ions are also responsible for driving chemistry in the cold (< 50 K) disk midplane. Ion-neutral reactions yield chemical complexity and life sustaining chemistry, particularly by creating formation pathways for organics (Cleeves et al. 2016) and water (van Dishoeck et al. 2013). If disks cannot efficiently form water, nascent planets would have to rely solely on inherited water from the parent molecular cloud (Cleeves et al. 2014). The efficiency of cold- water production may also vary with distance from the star, which would result in variations in ice across the disk. Understanding the distribution of ice is important, as the habitability of Earth-like planets may depend on post-formation delivery of water ice from asteroids and comets from the outer solar system. The distribution of ice also directly influences the atmospheric and core compositions of gas giants (Öberg et al. 2011).

Ionization in disks is driven by several different sources including X-rays, cosmic rays (CRs), and internal radiation from short-lived radionuclides (SLRs). In addition the diverse set of sources, each of these processes ionizes different vertical and radial regions of the disk (Figure 1). For example, X-rays are strong sources of ionization at the surface but have less of an effect as they are

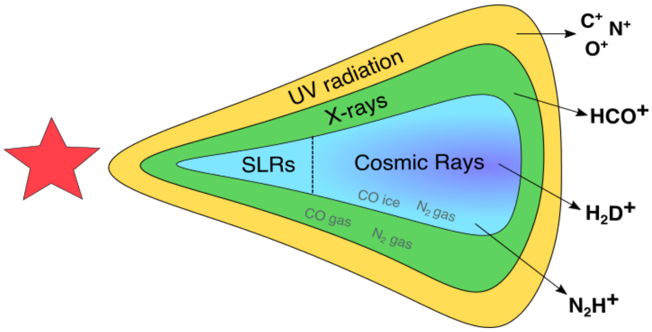

Figure 1. Dominant ionization processes and ionization tracing molecules for the distinct layers and radial zones in a typical protoplanetary disk.

attenuated through the disk. However, they may still have a significant impact in dense layers depending on the hardness of the stellar spectrum (Igea & Glassgold 1999). The most important sources of ionization in the planet–forming midplane region are less certain. For example, SLRs such as ^{36}Cl and ^{26}Al can be enriched in star forming environments recently polluted by supernovae. These species settle to the midplane of the disk and may provide some amount of ionization; however, their contribution to a "typical" disk remains relatively uncertain, especially since their abundance should vary between star forming regions (e.g., Adams et al. 2014). CRs are expected to be the most important sources of ionization in the most dense and cold regions of the disk where X-rays are strongly attenuated. The rate of CR ionization in the dense ISM is on the order of 10^{-17} s^{-1} but this rate could be reduced by orders of magnitude due to CR exclusion by stellar winds or magnetic fields (Cleeves et al. 2013, 2015) or enhanced due to local particle acceleration (Padovani et al. 2015, 2016). Ultimately, navigating this complex picture of ionization across the 2D disk environment requires a merging of theoretical dynamical and chemical models with reliable observational constraints.

In this work we look at several reliable ionization tracers, $HCO^+$and its isotopologue $H^{13}CO^+$, which are "surface tracers", and N_2H^+, a snowline tracer, in DM Tau. DM Tau is a particularly interesting test case for this study because it is the only disk known to have turbulence (Flaherty et al. 2020)- an important factor in regulating planet formation. We use a well-constrained physical structure of the disk and a 2D astrochemical code to model the abundances of the observed species across different levels of ionization and different chemical conditions. In the following sections we describe the methods and present preliminary results for a grid of 9 astrochemcial models for DM Tau. We then discuss the future application of these methods to 6 additional sources from the same sample, and to a large survey of 80 disks.

ALMA Observations

Observations of HCO^+ 4–3, N_2H^+ 4–3, and $H^{13}CO^+$ 3–2 were taken with ALMA under project code 2021.1.00138.S (PI: Cleeves). We performed continuum subtraction and line imaging using the uvcontsub and tclean commands from CASA 5.6.1. For the line imaging of HCO^+ we used Briggs weighting and a robust parameter of 0.5. The data for N_2H^+ was more noisy due to the line's close proximity to atmospheric water vapour features. We used natural weighting and a uvtaper of 0.5" when imaging the N_2H^+ 4–3 line in order to maximize sensitivity. Due to the high noise, we only use the integrated line flux for N_2H^+ 4–3 as a constraint, rather than comparing directly in the image plane. To help constrain N_2H^+ we utilize archival ALMA data of the 3–2 transition (project 2015.1.00678.S, PI: Qi) for comparison in the image plane. For all of our imaging we use keplerian masks (Teague 2020). Our final channel maps for 4–3, $H^{13}CO^+$ 3–2, and N_2H^+ 3–2 are shown in Figures 2-4.

Modeling DM Tau

Our physical model was developed using a combination of ALMA CO observations from Flaherty et al. (2020) and Submillimeter Array (SMA) dust continuum observations from Andrews et al. (2011). Previous physical models based on CO observations include only small dust grains (submicron). However, larger grains play an important role in setting midplane ionization because they shield the inner disk material from incident radiation. Since our work focuses on ionization in the disk it is particularly important that our physical model of the disk midplane include both small and large dust grains. Thus we present a physical model that includes large dust grains while maintaining sensitivity to the gas in the disk.

The "Frankenmodel" incorporates characteristics of the best–fit gas (Flaherty et al. 2020) and dust (Andrews et al. 2011) models for DM Tau. We use gas densities from the well-constrained Flaherty et al. (2020) model and incorporate large–grain dust densities calculated following the treatment in Andrews et al. (2011). Small– and large–grain dust densities were calculated starting with a global surface density profile,

$$\Sigma_g = \Sigma_c \left(\frac{R}{R_c}\right)^{-\gamma} \exp\left[-\left(\frac{R}{R_c}\right)^{2-\gamma}\right] \tag{1}$$

which was normalized using the dust mass from the Flaherty et al. (2020) model to yield the desired dust-to-gas

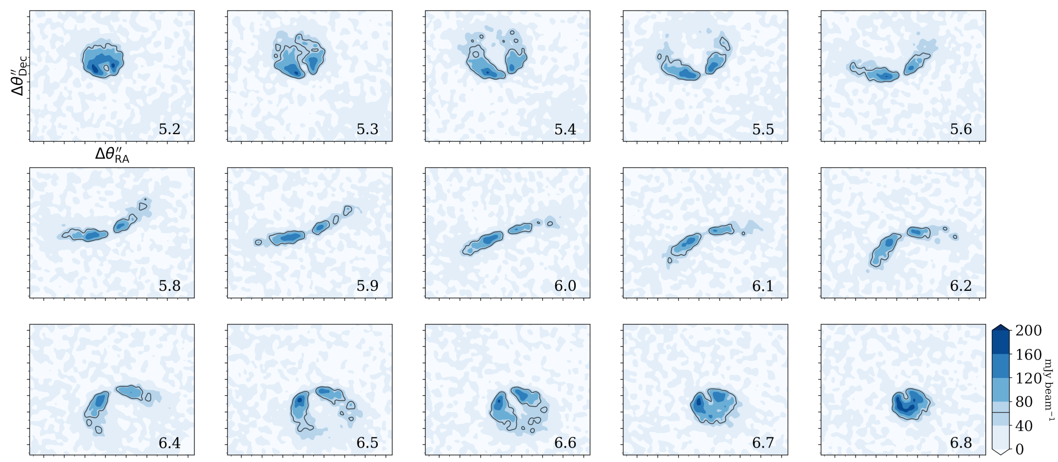

Figure 2. Channel map for DM Tau HCO^+ 4–3

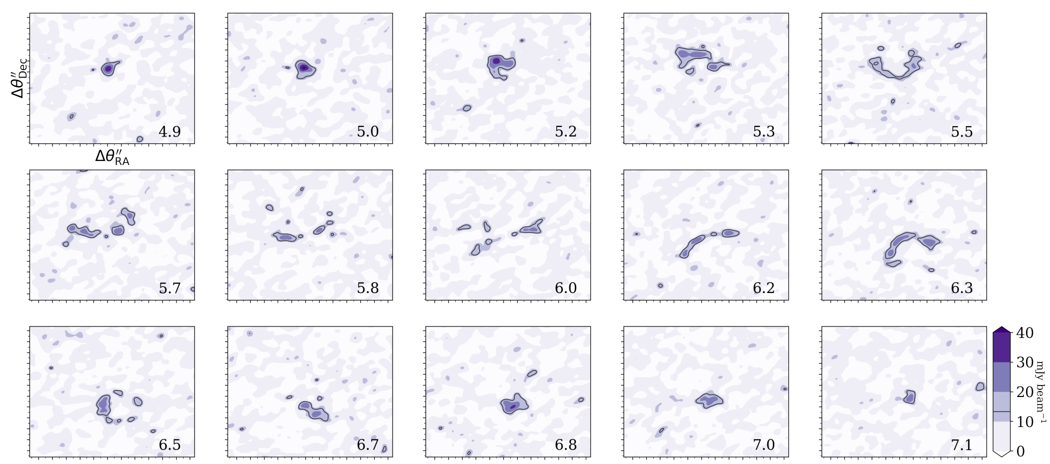

Figure 3. Channel map for DM Tau $H^{13}CO^+$ 3–2

ratio of 1:100. The characteristic scaling radius R_c was determined via parametric modeling and has a value of 135 au for DM Tau. The disk's 4 au inner dust ring and 20 au gap are simulated by depleting the dust by a factor $\delta_{cav} = 4.8$ in the region R < $R_{cav} = 19$. Values of δ_{cav} and R_{cav} come from parametric modeling and still match well to the latest observations confirming DM Tau's inner structure. With the resulting surface density profile we calculate dust densities for small and large grains using

$$\rho_s = \frac{(1-f)\Sigma}{\sqrt{2\pi}H} \exp\left[-\frac{1}{2}\left(\frac{z}{H}\right)^2\right] \quad (2)$$

and

$$\rho_l = \frac{(1-f)\Sigma}{\sqrt{2\pi}H\chi} \exp\left[-\frac{1}{2}\left(\frac{z}{\chi H}\right)^2\right] \quad (3)$$

where f (fraction of dust in large grains) and χ (power law index) are settling parameters fixed at 0.85 and 0.2 respectively, and H is the vertical scale height. We combine the two dust models by adding the large–grain dust densities to the existing small–grain densities from Flaherty et al. (2020) and include their fractional abundances for use in the physical and chemical modeling. Figure 5 shows the gas surface density profile and a comparison of the three dust surface density profiles. The Frankenmodel maintains the necessary dust-to-gas ratio ($\sim$ 1:100), allowing us to incorporate large–grains and a more accurate dust profile while continuing to utilize the most accurate gas densities and temperatures.

Model chemical abundances are calculated using a 2D time–dependent rate equation chemical code from Fogel et al. (2010). The results presented in this work make use of an updated chemical network, including

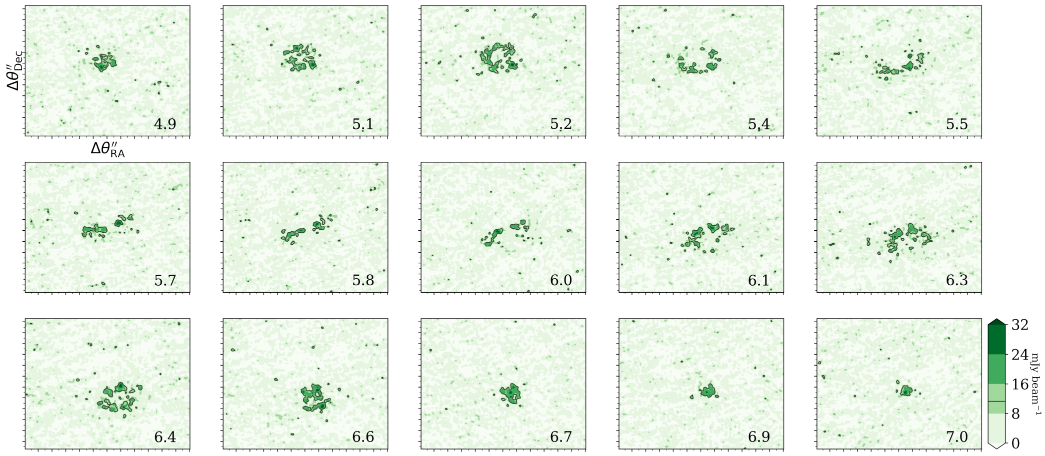

Figure 4. Channel map for DM Tau N_2H^+ 3–2

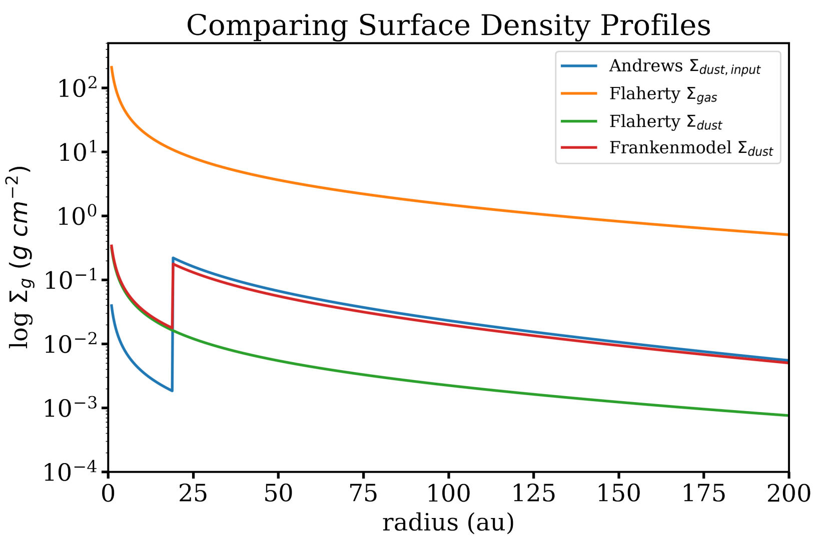

Figure 5. Surface density profiles for DM Tau from Flaherty et al. (2020) (gas in orange, dust in green) and Andrews et al. (2011) (dust in blue) alongside the combined "Frankenmodel" dust surface density profile (red).

deuterium isotopes and fractionation, with a total of 18,608 reactions.

Our chemical models include ionization from three sources: UV photons, X-ray photons, and CRs. We exclude effects of SLRs for now as their rate of ionization will have decayed over DM Tau's lifetime ($\sim$ 3.6 Myr) and ultimately should have negligible contributions at the disk's current age.

Since the observations reveal very faint N_2H^+ emission, we explored several avenues for reducing model emission of this species. N_2H^+ is produced via CR/X-ray driven reactions between diatomic nitrogen, N_2, and H_3^+, and is destroyed in the presence of CO, which reacts to form HCO^+. Thus, in order to reduce the production of N_2H^+ in our models we can 1) reduce CR and XR ionization, 2) increase the initial abundance of CO, or 3) reduce the initial abundance of N_2. Increasing CO works well to reduce N_2H^+ levels, but is unsupported by previous studies that have constrained the CO depletion in DM Tau to be 10 within the N_2H^+ emitting region (Zhang et al. 2019). With that in mind, we explore the other two axes: reduced CR/X-ray ionization and N_2 depletion. Since we expect CRs to be more influential over midplane chemistry, we begin by running a grid of models with three different CR ionization rates (ζ_{CR}) and three different initial N_2 abundances. The values and combinations of ζ_{CR} and n(N_2)/n(H) are listed in Table 1. We also explore an extreme model case where

ζ_{CR} (s^{-1})	$n(N_2)/n(H)$
2.0×10^{-17} (W98)	3.75×10^{-5}
1.6×10^{-19} (SSX)	7.50×10^{-6}
1.0×10^{-21} (TTX)	3.75×10^{-6}

Table 1. CR ionization rates (ζ_{CR}) and initial N_2 abundances for model grid, resulting in a total of 9 distinct models. The three ionization rates come from Webber (1998), the Solar System Maximum (Cleeves et al. 2013), and an extrapolated T Tauri Maximum (Cleeves et al. 2013), respectively.

there is no X-ray ionization, no CO depletion, and nitrogen is depleted.

Preliminary Model Results

Results from our grid of models (Figure 6) suggest that nitrogen depletion may be one factor contributing to the low midplane ionization, as traced by observations of N_2H^+. However, even with the lowest rate of CR ionization and a nitrogen depletion factor of 10, our model radial profile remains between a factor of 1-2x too bright.

Our models also overproduce $H^{13}CO^+$- the optically thin isotopologue of HCO^+. The fact that both $H^{13}CO^+$ and N_2H^+ are too bright in the models suggests that perhaps a physical ionization-reducing mechanism may be at play, rather than a purely chemical mechanism. At the same time, our model HCO^+ profiles are far too dim. This can be partially explained by the fact that HCO^+ is optically thick, so the observations may be tracing warmer gas than our model observations are, resulting in a brighter image. Still, we need some way of producing more HCO^+.

For the extreme case with no CO depletion and a factor of 10 N_2 depletion, we compare models with and without X-ray ionization (Figure 7). In these extreme N_2H^+ reduced conditions, we fall below observed values of N_2H^+ emission. Given these results, and previous work by Zhang et al. (2019) which suggests that DM Tau is in fact depleted in CO, we can rule out the "no CO depletion" models for good. Reduced X-ray ionization, along with depleted N_2, appears to be a plausible way of explaining DM Tau's low midplane ionization. Given that DM Tau has a large inner, it is possible that the dust at the edge of the gap has formed an opaque wall that blocks ionizing X-rays from reaching the midplane in the inner disk.

Future Applications with ALMA and JWST

Our forward modeling technique is useful for making detailed 2D constraints on ionization, as it allows us to explore a variety of factors impacting the ionization environment of an individual source. We are working to apply this method in a study of six additional sources, for which we have observations of HCO^+, $H^{13}CO^+$, $HC^{18}O^+$, N_2H^+, DCO^+, and H_2D^+. With multiple ionization tracing molecules and our 2D chemical model, we will be able to constrain these disks' ionization environments and better understand the chemical and physical processes related to planet formation.

For one of our sources, V4046 Sgr, we will use the resulting model and ionization constraints to predict the distribution of ice in the disk. Ice observations from JWST- the first of their kind in a protoplanetary disk- will be taken soon, allowing us to test our model predictions and synthesize the capabilities of ALMA, JWST, and chemical modeling.

Characterizing ionization in individual sources is a powerful tool for understanding the chemistry and physics at play in protoplanetary disks. However, drawing statistical conclusions regarding the planet–forming capabilities and conditions in the "average" PPD requires a large sample of disks. With the ongoing ALMA DECO Large Program, we have an opportunity to test our ability to constrain ionization across a large sample (80 disks) using only one ionization tracer, N_2H^+. By making statistical comparisons across the sample of disks we hope to determine relationships between disk ionization and various properties such as disk size and morphology. Overall, this work moves toward a deeper understanding of disk ionization and its connection to planet formation conditions and chemical composition.

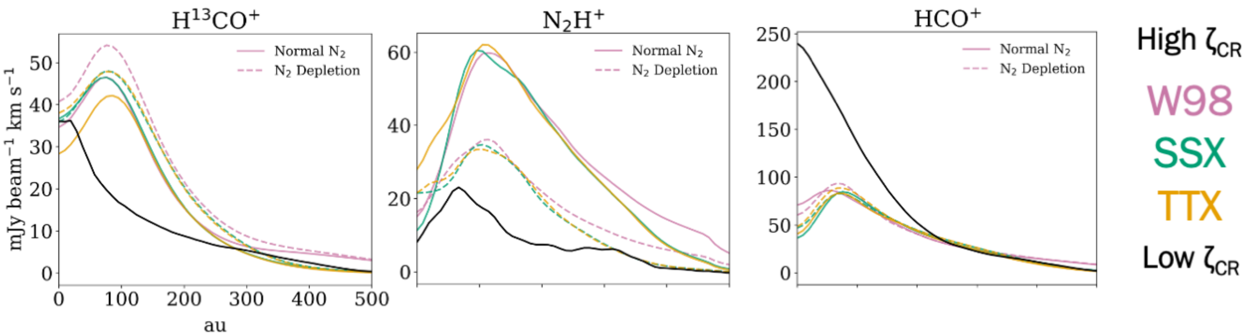

Figure 6. Observed emission profiles (solid black lines) vs. profiles of full-nitrogen and nitrogen-depleted models with three different values of ζ_{CR}.

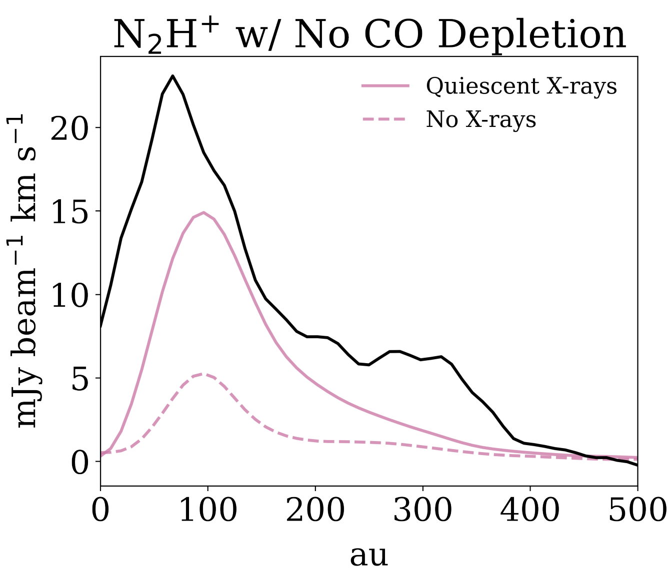

Figure 7. Observed emission profile (solid black line) vs. profiles of full-CO/N$_2$ depleted models with and without X-rays. These models share the same value of ζ_{CR} from Webber (1998).

REFERENCES

Adams, F. C., Fatuzzo, M., & Holden, L. 2014, ApJ, 789, 86, doi: 10.1088/0004-637x/789/1/86

Andrews, S. M., Wilner, D. J., Espaillat, C., et al. 2011, The Astrophysical Journal, 732, 42, doi: 10.1088/0004-637x/732/1/42

Balbus, S. A., & Hawley, J. F. 1991, ApJ, 376, 214, doi: 10.1086/170270

Batalha, N. M. 2014, Proceedings of the National Academy of Sciences, 111, 12647, doi: 10.1073/pnas.1304196111

Cleeves, L. I., Adams, F. C., & Bergin, E. A. 2013, ApJ, 772, 5, doi: 10.1088/0004-637X/772/1/5

Cleeves, L. I., Adams, F. C., & Bergin, E. A. 2013, The Astrophysical Journal, 772, 5, doi: 10.1088/0004-637x/772/1/5

Cleeves, L. I., Bergin, E. A., & Adams, F. C. 2014, ApJ, 794, 123, doi: 10.1088/0004-637x/794/2/123

Cleeves, L. I., Bergin, E. A., Qi, C., Adams, F. C., & Öberg, K. I. 2015, ApJ, 799, 204, doi: 10.1088/0004-637X/799/2/204

Cleeves, L. I., Öberg, K. I., Wilner, D. J., et al. 2016, ApJ, 832, 110, doi: 10.3847/0004-637X/832/2/110

Flaherty, K., Hughes, A. M., Simon, J. B., et al. 2020, ApJ, 895, 109, doi: 10.3847/1538-4357/ab8cc5

Fogel, J. K. J., Bethell, T. J., Bergin, E. A., Calvet, N., & Semenov, D. 2010, The Astrophysical Journal, 726, 29, doi: 10.1088/0004-637X/726/1/29

Igea, J., & Glassgold, A. E. 1999, ApJ, 518, 848, doi: 10.1086/307302

Okuzumi, S. 2009, The Astrophysical Journal, 698, 1122, doi: 10.1088/0004-637x/698/2/1122

Padovani, M., Hennebelle, P., Marcowith, A., & Ferrière, K. 2015, A&A, 582, L13, doi: 10.1051/0004-6361/201526874

Padovani, M., Marcowith, A., Hennebelle, P., & Ferrière, K. 2016, A&A, 590, A8, doi: 10.1051/0004-6361/201628221

Speedie, J., Pudritz, R. E., Cridland, A. J., Meru, F., & Booth, R. A. 2021, Monthly Notices of the Royal Astronomical Society, 510, 6059, doi: 10.1093/mnras/stab3180

Teague, R. 2020, richteague/keplerian_mask: Initial Release, 1.0, Zenodo, doi: 10.5281/zenodo.4321137

van Dishoeck, E. F., Herbst, E., & Neufeld, D. A. 2013, Chemical Reviews, 113, 9043, doi: 10.1021/cr4003177

Wang, J. J., Ginzburg, S., Ren, B., et al. 2020, AJ, 159, 263, doi: 10.3847/1538-3881/ab8aef

Webber, W. R. 1998, ApJ, 506, 329, doi: 10.1086/306222

Weidenschilling, S. J., & Cuzzi, J. N. 1993, in Protostars and Planets III, ed. E. H. Levy & J. I. Lunine, 1031

Zhang, K., Bergin, E. A., Schwarz, K., Krijt, S., & Ciesla, F. 2019, ApJ, 883, 98, doi: 10.3847/1538-4357/ab38b9

Öberg, K. I., Boogert, A. C. A., Pontoppidan, K. M., et al. 2011, The Astrophysical Journal, 740, 109, doi: 10.1088/0004-637x/740/2/109